Physics – Uspekhi **50** (11) 1171 – 1178 (2007)

FROM THE CURRENT LITERATURE

PACS numbers: **71.10. – w**, **71.27. + a**, **71.30. + h**, **73.40. – c**, 74.62.Dh

Colossal electroresistance and electron instability in strongly correlated electron systems

N A Tulina

DOI: 10.1070/PU2007v050n11ABEH006396

Contents

Abstract. Studies of the electron instability effects (EIEs) in structures based on strongly correlated electron systems (SCESs), such as high-temperature superconductors (HTSCs) and doped manganites (compounds with colossal magnetoresistance), are reviewed. These effects manifest themselves in a change of several orders of magnitude in the resistive state of the normal metal – HTSC or normal metal – DM (doped manganite) interface in an electric field under significant current injection conditions. The results of studying HTSC- and doped-manganite-based heterojunctions are considered. EIEs in heterostructures are compared with the electric field effect on the properties of an SCES in thin films and gate-containing devices. The general features and distinctions in the physics of these phenomena are analyzed.

1. Introduction

The effect of switching the resistive properties of heterojunctions, which is considered in this work, is correlated with the behavior of electronic devices (investigated in the 1960s) that are switched from one conducting state to another or oscillate between them at a certain applied voltage. These devices include tunnel diodes [2], Gunn diodes [3], avalanche diodes [4], thyristors [5], amorphous chalcogenide thin films [6], and dioxide VO_2 films [7]. As a rule, these switching devices are characterized by specific current – voltage characteristics (CVCs), namely, S-type (current-controlled) and N-type (voltage-controlled) characteristics [1]. The effects of the first type are related to the thermal effect of an electric current and the appearance of current domains or current pinching, and they are nonpolar. The second-type effects are caused by the effect of a band structure on the properties of semiconductor films. The field of studies in this early period is described in review [6].

Strongly correlated electron systems (SCESs), such as perovskite compounds based on the oxides of transition metals [high-temperature superconductors (HTSCs)], and doped manganites (DMs) are subjects of extensive study in modern physics [8 – 13] because of their transition into a superconducting state and colossal magnetoresistance (CMR), which are still incompletely understood. HTSCs and DMs are based on antiferromagnetic Mott dielectrics. A metallic state in these compounds is usually achieved upon doping by an alkaline-earth element or via a change in the oxygen content. Figures 1 – 3 show examples of the HTSC and doped $La_{1-x}Sr_xMnO_3$ manganite phase diagrams.

In these compounds, several degrees of freedom (spin, charge, spin – orbit, and phonon degrees) compete and interact with each other. Therefore, they exhibit a very wide class of phase transitions and are extremely sensitive to external actions, such as magnetic and electric fields and mechanical pressure. It was found that, as Mott systems, HTSCs and DMs can exist in the state of phase separation (PS) into dielectric (or semiconductor) and metallic phases under certain conditions (degree of doping, effect of electric and magnetic fields; see Fig. 4) [8 – 13]. PS regions for low doping are indicated in Figs 1 – 3.

The following two PS types are usually distinguished [9, 11, 12]: electron-induced PS, which is caused by the division of a free-charge system into areas with different carrier concentrations and results in a two-phase division into atomic-scale volumes [9, 10], and impurity-induced PS into phases several micrometers in size with the same electron density. Impurity-induced PS can be realized if the diffusion

N A Tulina Institute of Solid State Physics, Russian Academy of Sciences, 142432 Chernogolovka, Moscow region, Russian Federation
Tel. (7-496) 993 27 55. Fax (7-496) 524 97 01
E-mail: tulina@issp.ac.ru

Received 18 April 2007
Uspekhi Fizicheskikh Nauk **177** (11) 1231 – 1239 (2007)
DOI: 10.3367/UFNr.0177.200711d.1231
Translated by K V Shakhlevich; edited by A M Semikhatov

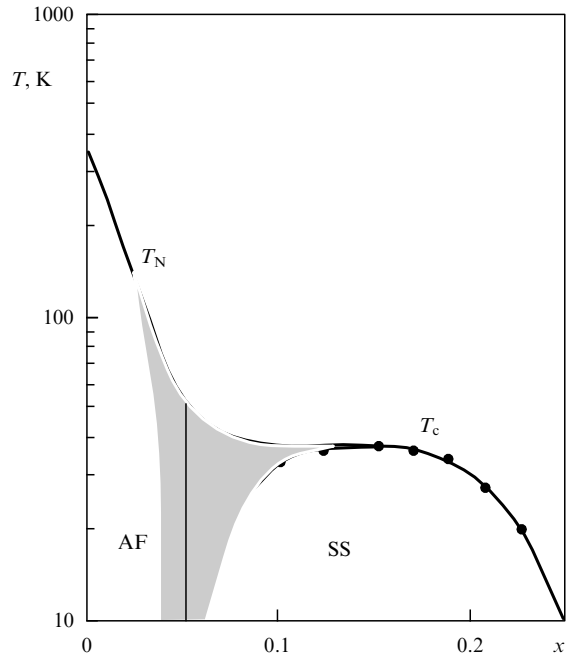

Figure 1. HTSC phase diagram [13]: AF, antiferromagnetic state; SS, superconducting state; T_N, Néel temperature; T_c, superconducting transition temperature. The two-phase region is shaded.

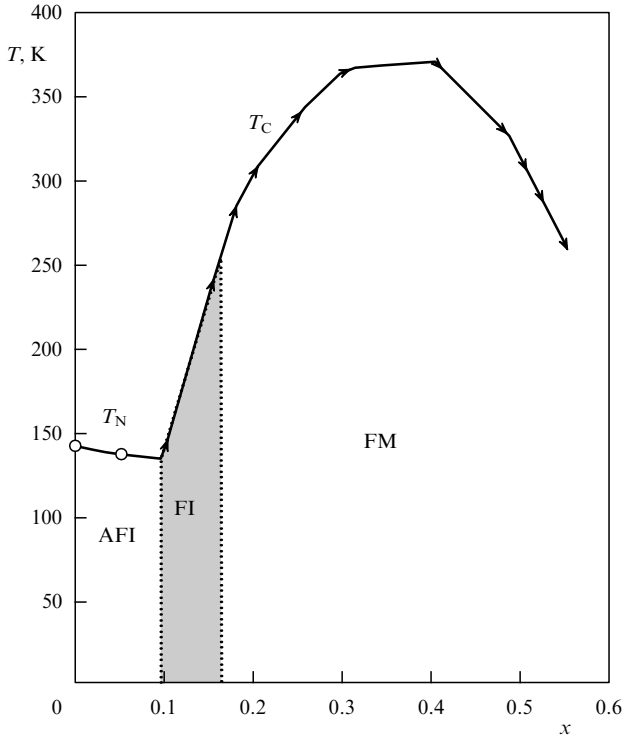

Figure 2. $La_{1-x}Sr_xMnO_3$ phase diagram [9]: FM, ferromagnetic metal; FI, ferromagnetic insulator, phase separation; AFI, antiferromagnetic insulator; T_C, Curie temperature. The two-phase region is shaded.

coefficient of the impurity is sufficiently high. Oxygen can be such an impurity in perovskite compounds based on the oxides of transition metals (i.e., HTSCs and DMs). Indeed, the diffusion coefficient of oxygen in a number of perovskites was experimentally found to be rather high ($\sim 10^{-9}$ cm^2 s^{-1} at room temperature).

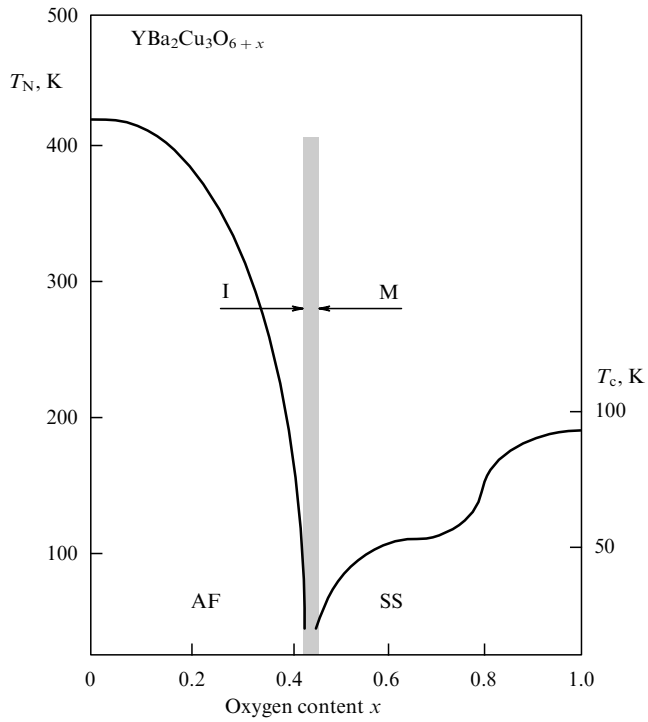

Figure 3. $YB_2Cu_3O_{6+x}$ phase diagram as a function of the oxygen content [14]: I, insulator with a tetragonal crystal structure; M, metal with an orthorhombic crystal structure. The two-phase region is shaded.

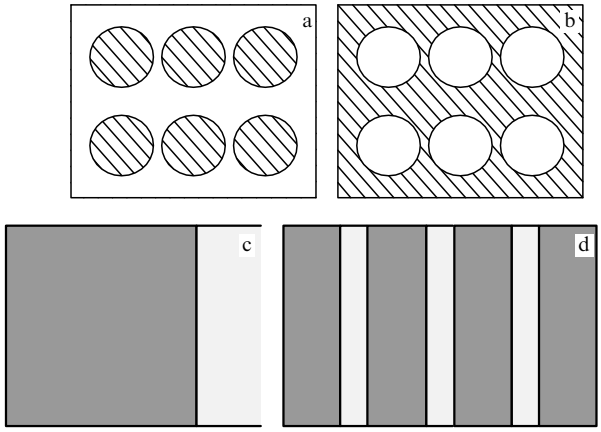

Figure 4. Types of phase separation [9]: (a) nonconducting state with metallic inclusions, (b) conducting state with dielectric inclusions, (c) macroscopic phase separation on the crystal surface, and (d) macroscopic stripe structures.

The presence of a two-phase state in manganites and HTSCs was detected and its evolution was studied by the following methods:

(i) structural methods (X-ray diffraction, neutron diffraction);

(ii) spectroscopic methods (nuclear magnetic resonance, ferromagnetic resonance, photoemission spectroscopy);

(iii) transport methods (the measurements of electron transport, magnetization, heat capacity, and thermal conductivity as functions of the magnetic field and temperature); and

(iv) the visualization of HTSCs and DMs in the PS state using magnetooptical methods, decoration, atomic-force microscopy, and scanning tunneling spectroscopy (Fig. 5).

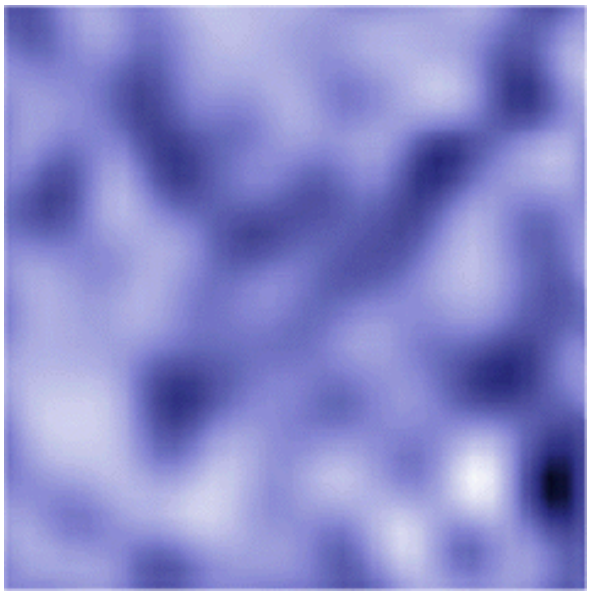

Figure 5. Microscopic electron inhomogeneity in superconducting BiSrCaCuO observed with scanning tunneling spectroscopy [15]. Bright areas (14 Å in size) are regions with a high local electron density of states.

SCES-based structures are thought to be promising for electronic-device elements. It is therefore interesting to study the electron instability effect (EIE) [i.e., colossal electroresistance (CER)] that is observed in heterostructures based on perovskite HTSC oxide compounds, ferroelectrics, perovskite Ti and Zr compounds, and doped manganites [16–28]. This effect manifests itself in a change of several orders of magnitude in the characteristics of the resistive state of the normal metal–HTSC or normal metal–DM interface in an electric field under significant current injection conditions. [1]

The EIEs detected in heterostructures are due to the processes occurring in the normal metal–doped manganite or normal metal–HTSC interface. These effects are polar, i.e., depend on the sign of the electric field applied to a heterostructure, and exhibit memory. On the one hand, EIEs can serve as a basis for memory devices; on the other hand, the behavior of EIEs is similar to that of SCESs, which opens up new opportunities for studying the microscopic nature of the main properties of such systems.

2. The electric field effect on the properties of structures based on strongly correlated electron systems

It is also necessary to distinguish the EIEs in heterojunctions from the electric field effect on the resistive properties of gate-containing devices and some DM films. In gate-containing devices, the currents are negligibly low, and an electric field changes the number of carriers (and, hence, the resistive properties of the structure) due to a change in the Coulomb interaction. Such effects have no memory and manifest themselves only in a high-strength electric field (Fig. 6).

These effects are determined by the screening length (Thomas–Fermi screening length) l_{TF}; for conventional superconductors and metals, it is very small (~ 1 Å) and depends on the number of carriers as

$$l_{TF} = \left(\frac{\varepsilon E_{F0}}{4\pi^2 e^2 n_0}\right)^{1/2},$$

where ε is the dielectric constant of the material and E_{F0} and n_0 are the Fermi energy and the carrier concentration in the absence of the electric field.

The carrier concentration in HTSCs and DMs is very low (of the order of 10^{21} cm^{-3}), and the number of carriers substantially affects the superconducting transition temperature in an HTSC, the Curie temperature in a DM, and their transport properties. For YBaCuO(123), $l_{TF} = 5-10$ Å; therefore, we can expect significant electric field effects on the superconducting and normal properties of HTSCs and DMs. The authors of a number of works detected the electric field effect on some properties of HTSCs. Specifically, an electric field increased the critical current in films [32–34], changed the excess current in Y–Ba–Cu–O–normal metal microcontacts [35], and induced an order–disorder transition on the surface of HTSCs [36]. YBaCuO samples were mainly used in such works (see [37–39]). Gate-containing structures were studied in several SCES compounds [40, 41].

The authors of [42] analyzed the electric field effect on the temperature dependence of the resistance of a three-terminal structure consisting of the LaBaMnO–Sr(TiNb)O p–n junction and a metallic electrode (Ag film). The transport properties of the p–n junction were studied as a function of the applied voltage (Fig. 7). The voltage across the gate is seen to radically change the transport properties and the Curie temperature (metal–insulator transition temperature) of the structure. This is a direct indication of a change in the phase state of $(LaBa)MnO_3$ as a result of the change in the number of carriers induced by an electric field. The authors of [42] believe that the degraded-layer depth in the p–n junction increases, which enhances the electric field effect. We note

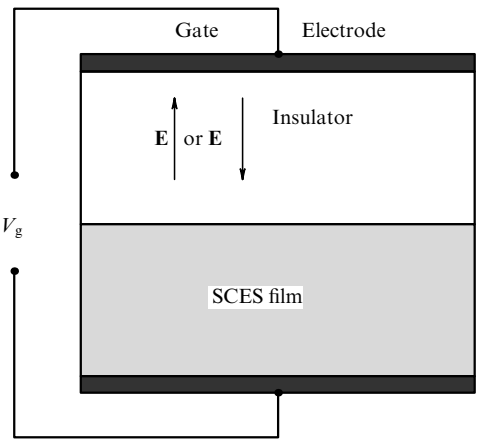

Figure 6. Schematic diagram of a gate-containing device designed to study the electric field effect on the properties of a superconducting film. V_g is the voltage across the gate.

[1] The term colossal electroresistance was introduced in [24], where DMs were studied, by analogy with the term colossal magnetoresistance (CMR), in order to designate a change in the electric resistance in a magnetic field. When a magnetic field is turned off, CMR is not retained; that is, CMR has no memory. In contrast to this behavior, the term CER (in [29–31], this effect is called giant electroresistance) is used for both the effects of a change in the electric resistance in an electric field in gate-containing films and devices and for EIE effects that change the resistive properties of structures and retain them after the electric field is turned off (see Section 4).

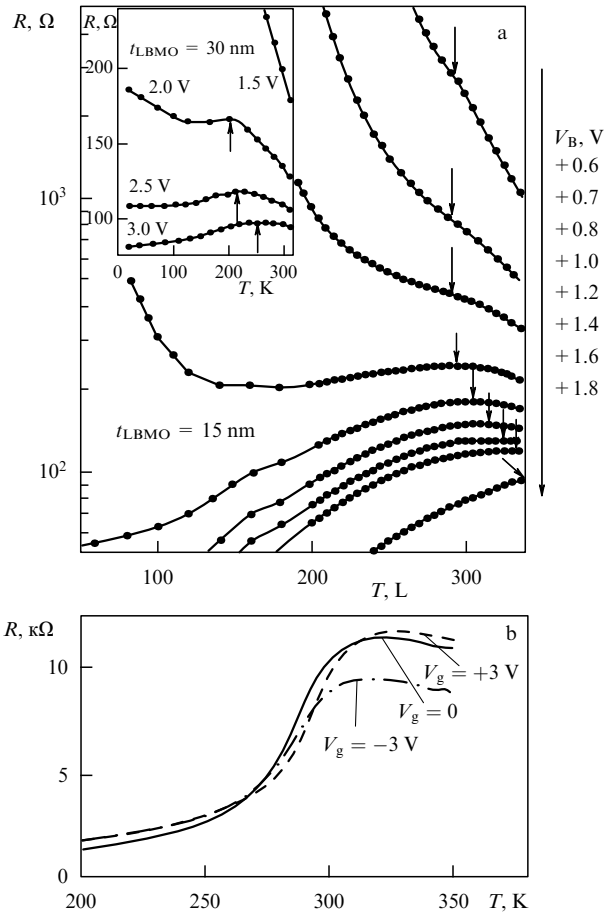

Figure 7. (a) Temperature dependences of the resistance of the p-(LaBa)MnO_3(15 nm)/n-Sr(TiNb)O_3 structure at various applied voltages [42]. The arrows indicate the metal – insulator transition temperature. The inset shows a similar dependence for a film of thickness t_{LBMO} = 30 nm. (b) The temperature dependence of resistance in the plane of a 10-nm-thick film at various voltages V_g across the gate in a transistor structure.

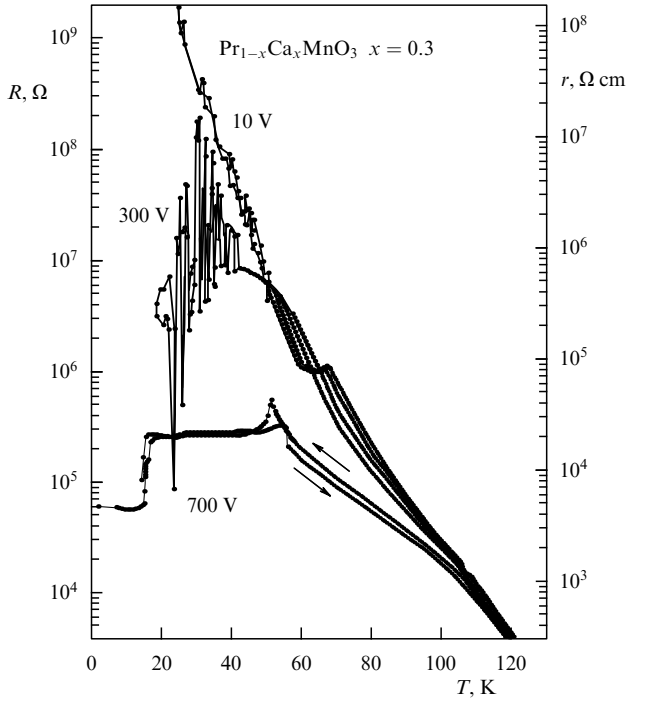

Figure 8. Temperature dependences of the resistance of a $Pr_{1-x}Ca_xMnO_3$ ($x = 0.3$) crystal at various applied voltages [45].

that the role of the degradation of the properties of HTSCs and CMR on the surface of single crystals investigated in [19, 43, 44] is very important. The authors of these works showed that a loss of oxygen leads to a change in the valent state of atoms on the surface of a single crystal and, hence, in the transport, superconducting, and magnetic properties of the material. In particular, the degradation of the surface of a DM results in a change in the Mn^{+3}/Mn^{+4} ratio, which determines the Curie temperature and transport properties of the interface [43].

3. The electric field effect on transport in the films and single crystals of strongly correlated electron systems

The effect of a direct current on the transport properties of manganites was studied in [29 – 31, 43, 46]. The dc-induced change in the character of the conductivity of DMs is most pronounced in the $Pr_{1-x}Ca_xMnO_3$ system [45]. The manganites of this family are nonconducting over the entire x range. As an electric voltage is applied, a single crystal undergoes a transition from a charge-ordered antiferromagnetic phase into a conducting ferromagnetic phase (Fig. 8).

Eerenstein et al. [31] detected a response of the phase state of a LaBaMnO film to the structural transition in the $BaTiO_3$ substrate. The results obtained demonstrate that internal stresses stimulate PS in a DM.

Gu et al. [47] theoretically considered the effect of the electric field of an electric current on a charge-ordered inclusion in a manganite medium subjected to phase separation. An electric field was assumed to concentrate at certain sites in the phase-separation medium. This field ($\sim 10^5$ V cm^{-1}) suppresses charge ordering, transforms the system from an antiferromagnetic into a ferromagnetic state, and stimulates the metal – insulator transition.

The effects described in this section are a direct confirmation of the Mott nature of SCESs, in which Coulomb interaction is suppressed by disordering, doping, and so on.

When researchers study the electron transport in a medium subjected to PS (DMs, HTSCs) under certain real conditions, they are dealing with the percolation transport of two resistor systems, namely, magnetically ordered (metallic) and charge-ordered (dielectric) systems, which form a complex structure in a film or single crystal. Thus, even a low electric field can significantly change the transport and magnetic properties of structures based on SCESs with PS. This state can be supported by the results in [48, 49], where the sign of CER was found to change as a function of the structural state of the matrix.

4. The electron instability effect in the heterostructures of strongly correlated electron systems

In this section, we consider experiments where researchers observed the effects of a radical change in the resistive properties of normal metal – doped manganite (HTSC) heterojunctions under significant current injection condi-

tions, when the phase state of the normal metal – SCES interface changed. These effects were named differently in different works:

(a) electric-field- and current-induced effects [16],

(b) the reproducible effect of resistive switching for application in memory-containing devices [18],

(c) electron instability effects [21],

(d) field-induced resistive switching [23],

(e) colossal electroresistance [24],

(f) giant resistive switching [26], and

(g) the electric-pulse-induced resistive change reversible effect [28].

This effect was first detected in heterojunctions in the form of BSCCO single crystal – Ag point contacts [16]. Similar effects were then observed in film structures [19 – 21]. In [18], this effect was detected in another perovskite system, i.e., a BSCCO – Ag film structure. This effect was found to be common to several classes of perovskite SCES compounds. This finding was supported when similar effects were revealed in doped manganites, which are related to HTSCs [20 – 28].

Although the current passing through a heterojunction plays a key role in the case under study, the detected switching effects differ from the effects of a change in the resistive properties of films and gate-containing devices (see Sections 2, 3), because the former effects exhibit memory. This behavior is reflected in the following transport properties of metastable states in heterojunctions:

• for the metallic state, (a) a linear $I(V)$ dependence and (b) metallic $R(T)$ dependence;

• for the paramagnetic state or phase separation, (a) a nonlinear $I(V)$ dependence and (b) activation contributions to the conductivity.

Figures 9 – 11 show examples of the current – voltage characteristics exhibiting EIEs and the temperature dependences of the resistances of the metastable phases in DM- and HTSC-based heterojunctions.

The phenomenon under study can be described as follows (Fig. 11a):

(1) An electric voltage, $-V$, is applied to a heterojunction (Fig. 11b, position *1*), and a high electric-field concentration is created upon microcontact (point) current spreading [21]. This field stimulates a phase transition into a carrier-depleted high-resistance phase (HRS, or off-state). The temperature dependence of the resistance and the CVC (branch *1 – 2*) of this phase are characteristic of systems with hopping resistance (localized carriers).

(2) At a certain voltage V_2 (position *2* in the CVC), the reverse phase transition into a low-resistance conducting phase (LRS, or on-state) occurs. This phase is characterized by a superconducting transition at $T = 85$ K. This low-resistance state is retained upon voltage sweeping up to negative voltages stimulating the reverse phase transition (branch *3 – 4*).

(3) CVC branches *1 – 2* and *3 – 4* are reversible; the states are switched in branches *2 – 3* and *4 – 5*.

(4) The resistance is determined by the single-crystal surface layer and is related to the predisposition of the SCES to phase separation into carrier-depleted and carrier-enriched regions under external actions.

The switching times determined in different works differ by several orders of magnitude. The shortest times, of the order of several picoseconds, have been detected in film devices [18, 26]. The authors of [19, 21] studied single crystals and observed slow processes, which were interpreted as

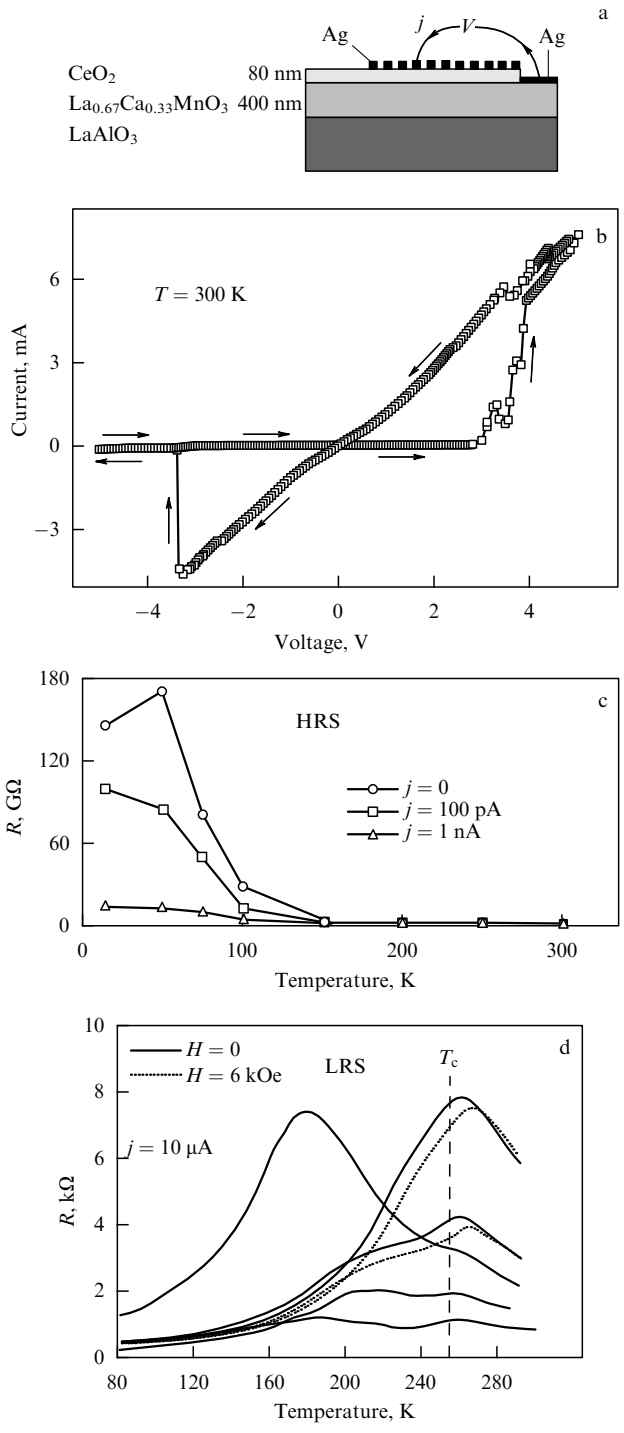

Figure 9. (a) Heteroepitaxial CeO_2(80 nm)/$La_{0.67}Ca_{0.33}MnO_3$(400 nm) film structure deposited onto an $LaAlO_3\langle 001\rangle$ single crystal in order to create a two-terminal device [26]. (b) Current – voltage characteristic of the Ag/CeO_2/$La_{0.67}Ca_{0.33}MnO_3$ heterojunction, which demonstrates reproducible switching between (c) the high-resistance state (HRS) with insulating properties and (d) the metallic state (LRS). The ratio of the resistances in these states is equal to 10^5. The reproducible electric switching represents a polar effect and manifests itself both upon slow voltage sweeping and under pulsed conditions.

oxygen diffusion through vacancies in a defect interface layer. Nian et al. [28] demonstrated resistive switching for a PrCaMnO – Ag film heterojunction under pulsed conditions at the pulse durations 300 and 100 ns (Fig. 10). However,

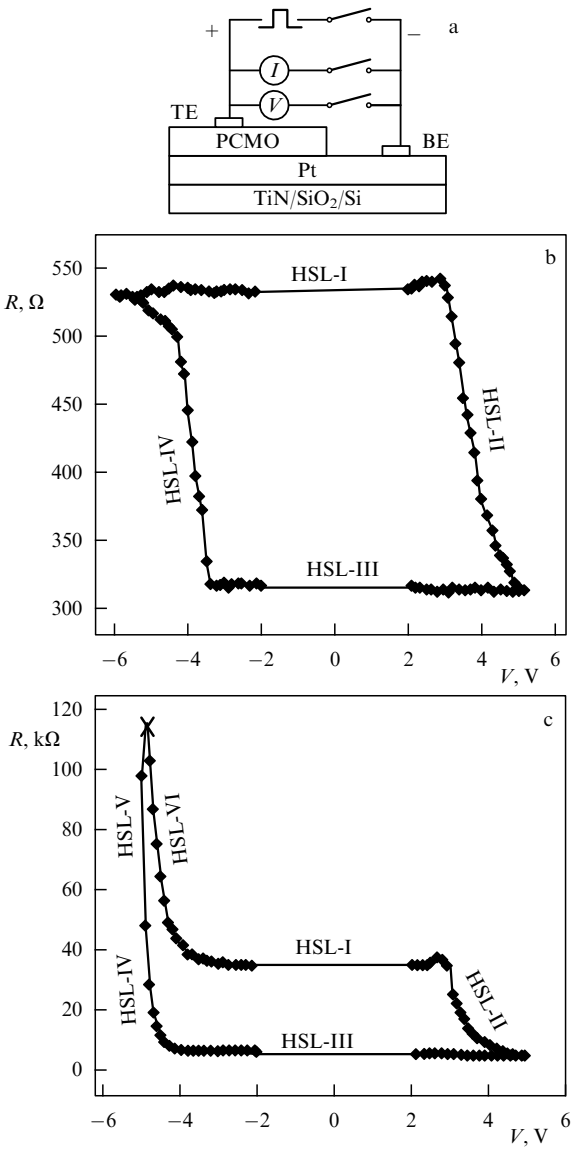

Figure 10. (a) Heterojunction schematic [27]. TE and BE are the top and bottom electrodes, respectively. (b, c) Resistive switching in a PrCaMnO – Ag film heterojunction under pulsed conditions for oxygen-rich and (b) oxygen-deficient films (c). V is the voltage pulse amplitude at the pulse duration 300 (b) and 100 ns (c); R is the heterojunction resistance; HSL-I is the low-resistance state of the heterojunction; HSL-III is the high-resistance state of the heterojunction; and HSL-II and HSL-IV are the intermediate states of the heterojunction.

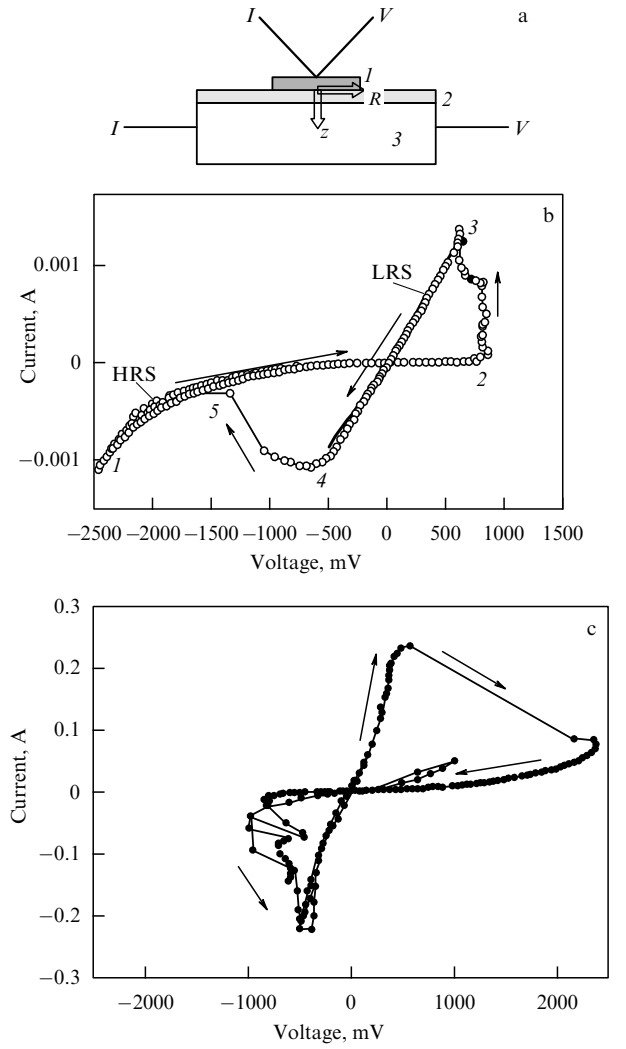

Figure 11. (a) Heterojunction schematic: (*1*) metallic electrode (silver needle or film), (*2*) surface degraded layer of a single crystal, and (*3*) single crystal. I and V are current and voltage supply. (b) CVC of the $Bi_2Sr_2CaCu_2O_{8+y}$ single crystal – Ag heterojunction with reproducible switching between LRS and HRS states [20]. The arrows indicate the voltage sweeping direction. The electric field $\mathbf{E}(\mathbf{J})$ is directed from the surface toward the bulk of the crystal when the sweep voltage is positive; $\mathbf{E}(\mathbf{J}) = \sigma\mathbf{J}$, where $\mathbf{J}$ is the current density and σ is the conductivity. (c) CVC of the $Ba_{0.6}K_{0.4}BiO_{3-x}$ – Ag single crystal – Ag heterojunction with reproducible switching between LRS and HRS states [52]. The arrows indicate the voltage sweeping direction. The electric field $-\mathbf{E}(\mathbf{J})$ is directed from the bulk of the crystal toward its surface when the sweep voltage is positive.

relaxation processes with times of several minutes were also detected in that work.

4.1 Model description of electron instability effects

There exist several model approaches to describing EIEs.

(1) In [22, 23], an electric field is assumed to produce oxygen defects at the interface, and the subsequent switching occurs due to the electrochemical migration of these defects.

(2) In [16, 19–21], a similar model, in which the heterojunction interface is regarded as an oxygen-degraded interlayer, is actually suggested. When a critical electric-field concentration is reached (the field is nonuniformly distributed over the heterojunction and has the highest concentration near the interface), oxygen and oxygen vacancies in the near-boundary layer are redistributed, which leads to PS in this layer and to a change in the resistive properties of the heterostructure. In [21], we numerically calculated the resistive properties of heterojunctions by taking the real resistive and thermal properties of HTSCs and manganites into account. Using numerical methods, we simultaneously solved the heat conduction and Poisson equations and calculated the electrodynamic and thermal properties of the heterojunctions in order to describe the electron instability effects in DM-based heterojunctions under strong current injection conditions. Comparison of the experimental and calculated data allows concluding that the effect of a transport current on the resistive properties of manganite-based and HTSC heterojunctions, observed in [19–21], causes impurity PS in the SCES. The motion of charged

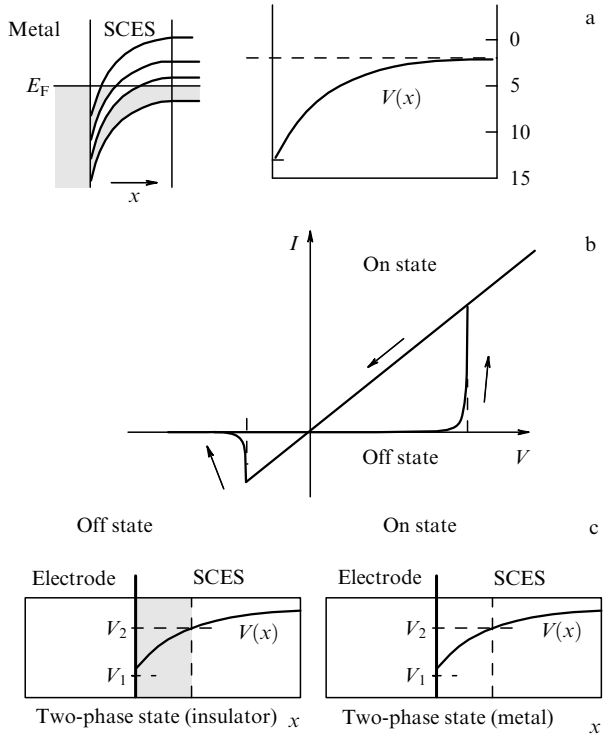

Figure 12. (a) Schematic diagram for the potential distribution over the metal–SCES interface [50]. (b) CVC of a metal–SCES structure in the model of [50]. (c) The off and on states of a metal–SCES structure.

oxygen ions in an electric field in the surface layer with a high oxygen-vacancy density favors PS.

(3) A heterojunction based on LaSrMnO with a dielectric CeO_2 interlayer was investigated in [26]. The authors assumed the existence of electric domains in the dielectric CeO_2 interlayer that interact with oxygen vacancies. An electric field moves the vacancies; as a result, the resistive states of the structure are switched.

(4) In [50], the EIE is assumed to be related to the nature of the Mott transition at the normal metal–SCES interface, where a two-dimensional structure, namely, metal/band insulator/metal/Mott insulator/SCES, forms (Fig. 12).

(5) The authors of [51] simulated the resistive switching effect in a polycrystalline manganite with spatially modulated oxygen vacancies.

Our analysis of these models demonstrates that electron instability effects are possible, first, due to the Mott nature of the metal–dielectric transition that occurs in the basic structures of the compounds considered. This transition is a first-order phase transition, exhibits a hysteresis, and allows the coexistence of two phases [50]. Second, a sufficiently high mobility of oxygen vacancies provides carrier redistribution in the transition formation region under the action of an electric field. However, it is obvious that the effects under study cannot be reduced to the electrodiffusion of oxygen ions, because EIEs are also detected at low temperatures [19, 21], where diffusion processes are slowed down.

4.2 Inversion of the electron instability effect in an electron-doped strongly correlated electron system

All the structures studied to investigate the EIE were mainly hole-doped SCESs. In [52], this effect was analyzed in heterostructures based on the electron-doped high-temperature superconductor $Ba_{0.6}K_{0.4}BiO_{3-x}$.

It was shown that the transport properties of the normal metal–$Ba_{0.6}K_{0.4}BiO_{3-x}$ single crystal interface depend on the polarity of the applied voltage and that switching into the high-resistance state occurs when the potential of the HTSC single crystal is negative with respect to the normal electrode (Fig. 11c). In this case, the current field $\mathbf{E} = \sigma\mathbf{J}$ is directed from the bulk of the crystal to *its surface*. In the case of switching detected in hole-doped HTSCs and DMs (which also exhibit hole conduction [16–28]), this effect had the opposite sign in the electric field. The change in the sign of the effect in electron-doped $Ba_{0.6}K_{0.4}BiO_{3-x}$ confirms the assumption that the electric field redistributes oxygen in the surface layer via a change in the number of vacancies, which differently affect the number of carriers in hole- and electron-doped perovskite structures.

The inversion of the resistive switching effect induced by a change in the type of carriers in a SCES that was detected in [52] supports the key role of charge effects and oxygen in the phenomena considered above.

4.3 Colossal electroresistance

Using model 4, we can estimate the resistive switching effect in terms of colossal electroresistance $\Delta R(V_{\rm off}, V_{\rm on})$,

$$\frac{\Delta R}{R} = \frac{R_{\rm off} - R_{\rm on}}{R_{\rm on}}\,,$$

where $R_{\rm off}$ is the resistance in the off-state and $R_{\rm on}$ is the resistance in the on-state,

$$\frac{\Delta R}{R} = \exp\left[\frac{\sqrt{2\varepsilon V_{\rm on}/(e\delta)}}{\xi}\right] - 1\,, \qquad (1)$$

$$\frac{\Delta R}{R} = \exp\left[\frac{\sqrt{2\varepsilon V_{\rm on}/(e\delta)} - \sqrt{2\varepsilon V_{\rm off}/(e\delta)}}{\xi}\right] - 1\,, \qquad (2)$$

where $V_{\rm off}$ is the voltage of switching into the off-state, $V_{\rm on}$ is the voltage of switching into the on-state, ξ is the decay length, and δ is the degree of SCES doping.

Equation (1) is valid for the switching between metallic and insulating states, and Eqn (2) is valid when none of the metastable states is metallic.

Figure 13 shows the dependence of the CER on the absolute value of the voltage $V_{\rm on}$ of switching from the off-state to the on-state that was obtained upon studying two related SCESs (HTSCs [16, 19, 52] and DMs [20, 21]) that had approximately the same level of doping δ. We used the absolute values of $V_{\rm on}$, because the voltage $Ba_{0.6}K_{0.4}BiO_{3-x}$ in electron-doped $V_{\rm on}$ had the opposite sign compared to the voltage in the hole-doped HTSC and DM. As can be seen from Fig. 13, there exists a significant scatter of the experimental data and Eqn (1) describes them inadequately. The overheating and electrodiffusion effects disregarded in model (4), which were investigated in detail in [21], are likely to contribute to the actual switching between the resistive states in heterojunctions.

5. Conclusion

Based on the results of studying the resistive switching effects in gate-containing devices, thin films, and SCES-based heterojunctions in electric and magnetic fields, we can distinguish the following common features for HTSCs and doped manganites, when they are regarded as Mott systems:

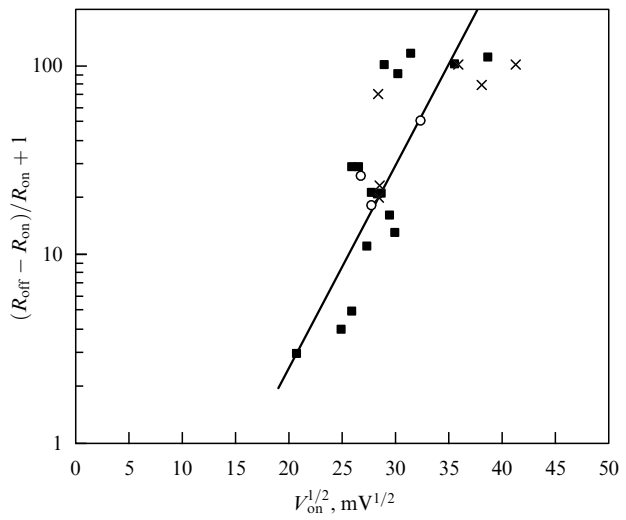

Figure 13. Colossal electrical resistance versus voltage V_{on} at which the off high-resistance state is switched to the on low-resistance metallic state [52]. The data for heterojunctions based on (circles) $Ba_{0.6}K_{0.4}BiO_3$, (X's) $La_{0.8}Ca_{0.2}MnO_{3-x}$, and (squares) $Bi_2Sr_2CaCu_2O_{8+x}$ single crystals.

(1) Their properties depend on the level of doping and the type of carriers.

(2) They undergo PS stimulated by various factors, namely, the level of doping, internal stresses, electric field, magnetic field, and so on.

(3) They contain mobile oxygen, which can move through vacancies in an electric field.

(4) They exhibit a hysteretic metal – insulator transition.

The existing model and theoretical descriptions incompletely accounts for all the processes that occur in the metal – SCES interface (i.e., oxygen diffusion, current-induced overheating, the type of carriers, etc.), form a potential distribution in the near-boundary region, and specify the times and character of resistive switching in SCES-based structures.

Acknowledgments. This work was supported by the Russian Foundation for Basic Research (project no. 05-02-17175a) and the Presidium of the Russian Academy of Sciences program New Materials.

References

1. Madan A, Shaw M P *The Physics and Applications of Amorphous Semiconductors* (San Diego: Academic Press, 1988) [Translated into Russian (Moscow: Mir, 1991)]
2. Esaki L *Phys. Rev.* **109** 603 (1958)
3. Gunn J B *IBM J. Res. Dev.* **8** 141 (1964)
4. Shockley W *Bell Syst. Tech. J.* **33** 799 (1954)
5. Fulop W *IEEE Trans. Electron. Dev.* **ED-10** 120 (1963)
6. Ovshinsky S R *Phys. Rev. Lett.* **21** 1450 (1968)
7. Andersson G *Acta Chem. Scand.* **8** 1599 (1959)
8. Dagotto E *Rev. Mod. Phys.* **66** 763 (1994)
9. Nagaev E L *Phys. Rep.* **346** 387 (2001)
10. Gor'kov L P *Usp. Fiz. Nauk* **168** 665 (1998) [*Phys. Usp.* **41** 589 (1998)]
11. Coey J M D, Viret M, von Molnár S *Adv. Phys.* **48** 167 (1999)
12. Dagotto E, Hotta T, Moreo A *Phys. Rep.* **344** 1 (2001)
13. Burgy J et al. *Phys. Rev. Lett.* **87** 277202 (2001)
14. Pickett W E et al. *Science* **255** 46 (1992)
15. Pan S H et al. *Nature* **413** 282 (2001)
16. Tulina N A, Emelchenco G A, Kulakov A B *Phys. Lett. A* **204** 74 (1995); Tulina N A *Physica C* **333** 214 (2000)
17. Watanabe Y *Phys. Rev. B* **59** 11257 (1999)
18. Beck A et al. *Appl. Phys. Lett.* **77** 139 (2000)
19. Tulina N A, Ionov A M, Chaika A N *Physica C* **366** 23 (2001)
20. Tulina N A et al. *Europhys. Lett.* **56** 836 (2001)
21. Tulina N A et al. *Physica C* **385** 563 (2003); Tulina N A, Sirotkin V V *Physica C* **400** 105 (2004)
22. Baikalov A et al. *Appl. Phys. Lett.* **83** 957 (2003)
23. Tsui S et al. *Appl. Phys. Lett.* **85** 317 (2004)
24. Odagawa A et al. *Phys. Rev. B* **70** 224403 (2004)
25. Rozenberg M J, Inoue I H, Sánchez M J *Phys. Rev. Lett.* **92** 178302 (2004)
26. Fors R, Khartsev S I, Grishin A M *Phys. Rev. B* **71** 045305 (2005)
27. Sawa A et al. *Appl. Phys. Lett.* **85** 4073 (2004)
28. Nian Y B et al. *Phys. Rev. Lett.* **98** 146403 (2007); Liu S Q, Wu N J, Ignatiev A *Appl. Phys. Lett.* **76** 2749 (2000)
29. Sun J Z *J. Magn. Magn. Mater.* **202** 157 (1999)
30. Debnath A K, Lin J G *Phys. Rev. B* **67** 064412 (2003)
31. Eerenstein W et al. *Nature Mater.* **6** 348 (2007); cond-mat/0609209
32. Xi X X et al. *Phys. Rev. Lett.* **68** 1240 (1992)
33. Mannhart J *Mod. Phys. Lett. B* **6** 555 (1992)
34. Matsui K et al. *Jpn. J. Appl. Phys.* **31** L1342 (1992)
35. Rybal'chenko L F et al. *Fiz. Nizk. Temp.* **17** 202 (1991) [*Sov. Low. Temp. Phys.* **17** 105 (1991)]
36. Bozhko S I,Tsoi V S *Physica C* **197** 362 (1992)
37. Nakajima K et al. *Appl. Phys. Lett.* **63** 684 (1993)
38. Chandrasekhar N, Valls O T, Goldman A M *Phys. Rev. Lett.* **71** 1079 (1993)
39. Grigelionis G, Tornau E E, Rosengren A *Phys. Rev. B* **53** 425 (1996)
40. Hasegawa T et al. *Phys. Rev. B* **69** 245115 (2004)
41. Ahn C H, Triscone J-M, Mannhart J *Nature* **424** 1015 (2003)
42. Tanaka H, Zhang J, Kawai T *Phys. Rev. Lett.* **88** 027204 (2001)
43. Chaika A N et al. *J. Electron Spectrosc. Relat. Phenom.* **148** 101 (2005)
44. Kim D S et al. *J. Appl. Phys.* **100** 093901(2006)
45. Asamitsu A et al. *Nature* **388** 50 (1997)
46. Yuzhelevski Y et al. *Phys. Rev. B* **64** 224428 (2001)
47. Gu R Y, Wang Z D, Ting C S *Phys. Rev.* **67** 153101 (2003)
48. Sun Y H et al. *J. Magn. Magn. Mater.* **311** 644 (2007)
49. Tulina N A et al., in *Poryadok – Besporyadok i Svoistva Oksidov*: *Sb. Trudov Mezhdunar. Simpoziuma, 2006 g., Sochi* (Proc. Int. Symposium on Order – Disorder and the Properties of Oxides, 2006, Sochi)
50. Oka T, Nagaosa N *Phys. Rev. Lett.* **95** 266403 (2005)
51. Quintero M et al. *Phys. Rev. Lett.* **98** 116601 (2007)
52. Tulina N A, Klinkova L A *Zh. Eksp. Teor. Fiz.* **132** 268 (2007) [*JETP* **105** 238 (2007)]